THE ASTROPHYSICAL JOURNAL, 437:465–475, 1994 December 10


# PROPERTIES AND VARIABILITY OF THE STELLAR WIND FROM P CYGNI

S. SCUDERI[1]
Istituto di Astronomia, Università di Catania, Viale Andrea Doria 6, I-95125, Catania, Italy; and Space Telescope Science Institute
G. BONANNO AND D. SPADARO
Osservatorio Astrofisico di Catania, Viale Andrea Doria 6, I-95125, Catania, Italy
N. PANAGIA[2]
Space Telescope Science Institute, 3700 San Martin Drive, Baltimore, MD 21218; and University of Catania
AND
H. J. G. L. M. LAMERS AND A. DE KOTER
SRON Laboratory for Space Research, Sorbonnelaan 2, 3584 CA Utrecht, The Netherlands; and Astronomical Institute, University of Utrecht, Princetonplein 5, Utrecht, The Netherlands
*Received 1993 June 28; accepted 1994 June 9*

## ABSTRACT

We present the results of a study of the wind of the luminous blue variable star P Cyg. We obtained spectroscopy of P Cyg in the Hα line region in the period 1988 June through 1991 July. We also used *UBV* photometric data to obtain information on the variations of the radius and of the effective temperature of the star. The properties of the wind of P Cyg at the different epochs of observations were determined by fitting theoretical Hα profiles to the observed ones. The computation of the theoretical profiles was done using the method of Scuderi et al. (1992), enhanced to include the effect of Thomson scattering by free electrons on the Hα profile. We found that the wind velocity field displays both systematic and irregular variations which match the variability of the stellar radius and effective temperature. On the other hand, the mass-loss rate is virtually constant, at a level of $(1.9 \pm 0.2) \times 10^{-5}\ M_\odot\ \mathrm{yr}^{-1}$, and so is the bolometric luminosity of the star. These results suggest that the mass-loss rate of P Cyg is determined entirely by internal properties of the star and is connected with its energy output whereas the wind velocity structure is also sensitive to even small changes of the photosphere conditions.

*Subject headings:* line: profiles — stars: atmospheres — stars: individual (P Cygni) — stars: mass loss

## 1. INTRODUCTION

The star P Cyg (HD 193237; B1 $Ia^+$) is the prototype of the class of the so-called P Cygni stars or luminous blue variables (LBV's). These stars are extremely luminous ($L \geq 10^{5.5}\ L_\odot$), display variability in their optical spectra, and have bright optical emission lines, often with P Cygni profiles. The stars are believed to be close to their Eddington limit, after they have evolved away from the main sequence (e.g., Lamers & Fitzpatrick 1988) and are characterized by high mass-loss rates, typically 10 times higher than those found for normal supergiants (e.g., Lamers 1987).

The main properties of P Cyg are as follows.

1. It has a visual magnitude of 4.9, with small ($\Delta V \simeq 0.2$ mag) irregular variations.

2. Its optical spectrum is characterized by emission lines with blue displaced absorption components indicating an outward expansion of circumstellar material. The rate at which P Cyg loses mass is about $1\text{–}2 \times 10^{-5}\ M_\odot\ \mathrm{yr}^{-1}$, as deduced from radio (Abbott, Bieging, & Churchwell 1981), infrared (Barlow & Cohen 1977; Felli et al. 1985), and Hα (Scuderi et al. 1992) observations.

3. The terminal velocity of the wind is about 200 km $\mathrm{s}^{-1}$ (Lamers, Korevaar, & Cassatella 1985). This velocity is much smaller than the terminal velocities found for typical B1 supergiants ($v_\infty \simeq 1500$ km $\mathrm{s}^{-1}$) (Gathier, Lamers, & Snow 1981; Prinja, Barlow, & Howarth 1990).

4. The stellar parameters of P Cyg have been derived by Lamers, de Groot, & Cassatella (1983) and are confirmed in a recent study by Pauldrach & Puls (1990): $\log (L/L_\odot) = 5.86 \pm 0.10$; $T_{\mathrm{eff}} = 19300 \pm 700$ K; $R/R_\odot = 76 \pm 8$ and $E(B-V) = 0.63 \pm 0.05$.

5. Variability is observed in both the continuum and in the profiles of optical (de Groot 1969 and this paper) and ultraviolet (Lamers et al. 1985) lines, but no definite periodicity has been found so far (Van Gent & Lamers 1986).

Since the winds from early-type stars are almost fully ionized and may absorb a sizable fraction of the Lyman continuum ionizing radiation (e.g., Felli & Panagia 1981), stellar winds are strong sources of recombination lines and, in particular, Hα. In fact, pioneering work on the Hα emission from stellar winds (Klein & Castor 1978; Ebbets 1982; Leitherer 1988) has already shown its great potential for the study of the mass loss from early-type stars. This potential has been confirmed by Scuderi et al. (1992). In fact, the Hα line provides one of the best tools to study the mass loss from early-type stars and its variability.

For this reason we are carrying out at the Catania Astrophysical Observatory a program of systematic spectroscopic observations of P Cyg in the Hα region, in order to study the time variability of the mass-loss process in this star.

We complement our spectroscopy with *UBV* photometry which provides information on the temporal behavior of the radius and of the effective temperature of P Cyg.

[1] ESA Fellow.
[2] Affiliated with the Astrophysics Division of the Space Science Department of ESA.

Here, we report on the results obtained in the period 1988 June–1991 July. By using new model calculations and fitting the observed Hα profiles, we determine the mass-loss rate and the velocity structure of the wind of P Cyg, at different epochs.

## 2. OBSERVATIONS AND DATA REDUCTION

### 2.1. *Spectroscopic Data*

All of the P Cyg spectra analyzed in this paper were obtained using the same instrumentation as described in Scuderi et al. (1992). It basically consists of an echelle spectrograph and a CCD detector attached to the 91 cm Cassegrain telescope of the Catania Astrophysical Observatory at Serra La Nave. The system was used in its low-dispersion mode ($\lambda/\Delta\lambda \simeq 7000$), so as to cover a wavelength interval of 450 Å, centered on the Hα line, with a spectral resolution of 0.89 Å which corresponds to about 40 km $s^{-1}$ in the Hα region (see Scuderi et al. 1992).

The spectroscopic observations of P Cyg presented here cover the period 1988 June–1991 July. A signal-to-noise ratio of about 50 in the continuum and of about 200 in the Hα line was achieved for all of the collected spectra.

The stellar spectra, calibrated in wavelength, were obtained from the CCD camera images as in Scuderi et al. (1992). The wavelength scale was corrected for the motion of the Earth and the radial velocity of P Cyg with respect to the Sun (−16 km $s^{-1}$; de Groot 1969). On each night we observed P Cyg at least twice, on a timescale of a few minutes. Since no appreciable variability was ever detected on such a timescale, we averaged the spectra relative to each night, in order to improve the S/N ratio.

To analyze the average spectra, we first normalized the stellar continuum to a unity level using the NOAO/IRAF package. Some examples of Hα normalized profiles are shown in Figure 1. Significant differences between spectra taken at different epochs are clearly seen in the line peak intensity as well as in the strength and the width of the line wings. Moreover, we see that a higher peak intensity is correlated to stronger and broader line wings.

The equivalent width of the Hα line was measured on the normalized spectra. The accuracy of these determinations is limited by uncertainties in the measured flux and, more importantly, by uncertainties in the definition of the level of the continuum (typically of the order of 2% of the continuum flux). The estimated relative error in the equivalent widths of the Hα line is 4%.

### 2.2. *Photometric Data*

*UBV* photometry of P Cyg has been obtained from two sources: observations by Percy and colleagues (Percy et al. 1988) and observations from the Phoenix-10 Automatic Photometric Observatory atop Mount Hopkins. The latter data were kindly provided to one of us (A. d. K.) by Mart de Groot and Mike Seeds. The observations cover the period from JD 2,445,841 to 2,448,236. The two sets of observations were combined and corrected for small systematic differences in order to obtain a homogeneous data set. The data were binned into 1 day intervals. The reduction of the *UBV* photometry of P Cyg and of other LBVs will be described elsewhere by Scholten et al. (1994). The accuracy of the measurements is about 0.03 mag in $V$ and 0.01 mag in $U-B$ and $B-V$.

The *UBV* photometry is not always simultaneous to our spectroscopy and also does not cover the entire period covered by the spectroscopic observations. Therefore, for some epochs the photometric data had to be interpolated, or extrapolated,

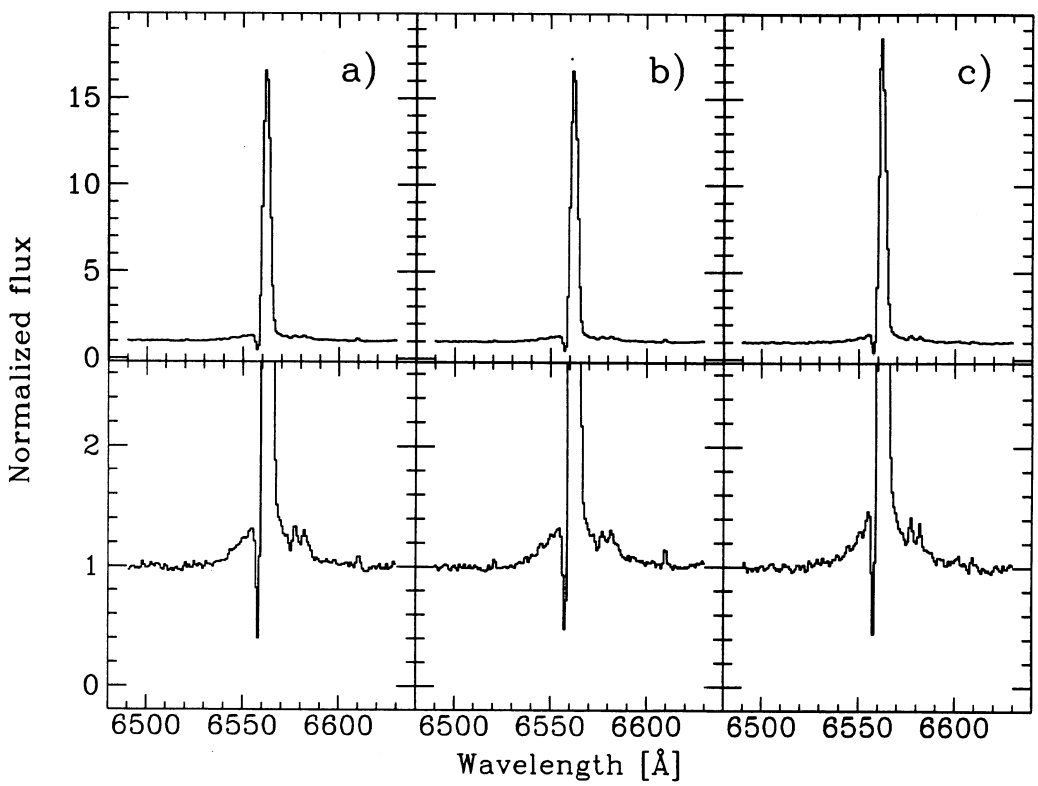


FIG. 1.—Hα normalized profiles obtained on (*a*) 1989 October 5, (*b*) 1990 August 9, and (*c*) 1991 July 23

from the actual observations. Some discussion of the procedure employed is given in § 4.4.3.

## 3. ANALYSIS OF THE OBSERVATIONS

### 3.1. *Equivalent Widths*

Table 1 lists the Hα equivalent widths and their uncertainties for the various epochs. The $W_{eq}$ values vary between about −86 Å and −67 Å, thus exhibiting variations much in excess of the observational uncertainties of about ±3 Å. The equivalent widths are plotted as a function of time (Julian date) in Figure 2. We notice significant variability in the equivalent width of the Hα line which is straightforward evidence of variability of the wind of P Cyg, already noticed by de Groot (1969) and Lamers et al. (1985).

The figure suggests a trend of a steady increase of the equivalent width with time, accompanied by more erratic, but significant variations on the day timescale.

In order to detect possible periodicity in the Hα equivalent width variations, we analyzed the data taken between 1988 June and 1991 July by means of a Fourier transform procedure (e.g., Scargle 1982) including also the data published by Taylor et al. (1991). Since their equivalent width estimates include only the contribution of the line core, we have corrected their values for an average contribution of the wings to the total equivalent width of 11%. We found no significant periodicity (for amplitudes higher than 5% of the average) over the 3 yr (1988 June through 1991 July) for which we have Hα line observations.

### 3.2. *Profiles*

To determine the physical parameters of the wind of P Cyg (temperature, density structure, velocity field, mass-loss rate) at the various epochs, we fitted theoretical Hα profiles, computed as described in Scuderi et al. (1992), to the observed profiles.

TABLE 1

Hα Equivalent Widths and Parameters of the Fit

| Date | J.D. (2,440,000+) | $-W_{eq}$ $\Delta W_{eq}$ (Å) | $v_0$ (km s$^{-1}$) | $\tau_0$ | $\tau_e$ |
|---|---|---|---|---|---|
| 1988 Jul 5 | 7348 | 77.6 ± 3.1 | 56 | 286 | 0.55 |
| 1988 Jul 10 | 7353 | 71.5 ± 2.9 | 51 | 302 | 0.46 |
| 1989 Jun 13 | 7691 | 73.6 ± 2.9 | 58 | 251 | 0.38 |
| 1989 Jun 15 | 7693 | 78.0 ± 3.1 | 54 | 313 | 0.42 |
| 1989 Sep 20 | 7790 | 74.9 ± 3.0 | 56 | 272 | 0.44 |
| 1898 Sep 21 | 7791 | 73.8 ± 2.9 | 56 | 264 | 0.46 |
| 1989 Sep 25 | 7793 | 72.8 ± 2.9 | 56 | 256 | 0.44 |
| 1989 Sep 27 | 7797 | 74.0 ± 3.0 | 54 | 287 | 0.44 |
| 1989 Oct 2 | 7802 | 71.8 ± 2.9 | 58 | 236 | 0.44 |
| 1989 Oct 5 | 7805 | 69.4 ± 2.8 | 55 | 244 | 0.44 |
| 1989 Oct 6 | 7806 | 71.1 ± 2.8 | 58 | 237 | 0.44 |
| 1989 Oct 10 | 7810 | 75.9 ± 3.0 | 55 | 287 | 0.44 |
| 1989 Nov 22 | 7853 | 73.4 ± 2.9 | 55 | 270 | 0.38 |
| 1989 Dec 14 | 7875 | 77.4 ± 3.1 | 54 | 311 | 0.46 |
| 1989 Dec 29 | 7890 | 80.8 ± 3.2 | 61 | 268 | 0.44 |
| 1990 Jan 16 | 7908 | 66.9 ± 2.7 | 56 | 228 | 0.38 |
| 1990 Aug 8 | 8112 | 75.9 ± 3.0 | 60 | 246 | 0.36 |
| 1990 Aug 9 | 8113 | 77.4 ± 3.1 | 58 | 270 | 0.38 |
| 1990 Aug 10 | 8114 | 73.6 ± 2.9 | 59 | 245 | 0.33 |
| 1990 Aug 11 | 8115 | 73.8 ± 2.9 | 57 | 259 | 0.33 |
| 1990 Aug 23 | 8127 | 73.1 ± 2.9 | 61 | 227 | 0.36 |
| 1990 Aug 24 | 8128 | 72.0 ± 2.9 | 61 | 220 | 0.36 |
| 1991 Jul 22 | 8460 | 82.8 ± 3.3 | 50 | 390 | 0.49 |
| 1991 Jul 23 | 8461 | 81.5 ± 3.3 | 51 | 378 | 0.46 |
| 1991 Jul 24 | 8462 | 79.1 ± 3.2 | 51 | 350 | 0.46 |
| 1991 Jul 26 | 8464 | 86.1 ± 3.4 | 50 | 423 | 0.52 |
| 1991 Jul 29 | 8467 | 80.7 ± 3.2 | 51 | 369 | 0.52 |

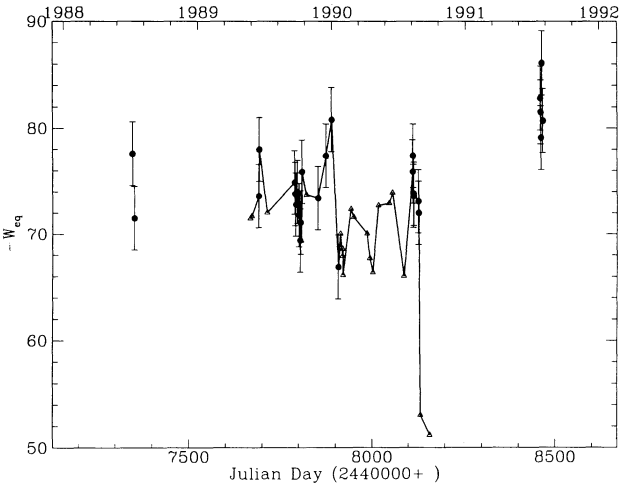


FIG. 2.—Hα equivalent width as a function of time. Filled dots correspond to the data obtained in this paper, triangles to those obtained by Taylor et al. (1991).

In particular, we have adopted the wind model as defined by Panagia & Felli (1975), Felli & Panagia (1981), and Panagia (1988). Hα profiles are calculated for a stationary, spherically symmetric, fully ionized, isothermal wind. The velocity field is assumed to have a truncated power-law dependence with radius

$$v(r) = v_0\left(\frac{r}{R_0}\right)^{\gamma}, \quad \frac{r}{R_0} \le \left(\frac{200}{v_0}\right)^{1/\gamma}$$
$$v(r) = 200, \quad \frac{r}{R_0} > \left(\frac{200}{v_0}\right)^{1/\gamma}, \tag{1}$$

where $v$ is in km s$^{-1}$ and $R_0$ is the lower boundary of the Hα emitting region. This velocity law starts with $v(R_0) = v_0$ and reaches a maximum of 200 km s$^{-1}$. We will show below that the profiles calculated with this truncated velocity law give a very good fit to the observed profiles for $v_0 \approx 55$ km s$^{-1}$ and $\gamma = 0.5$.

An inspection to the observed profiles reveals that in all cases the energy which may be emitted exclusively by layers moving at velocities lower than 55 km s$^{-1}$ is equal or less than the experimental error of 4%. We can use this result to constrain the possible values of the inner radius of the emitting region. Since the Hα line in P Cyg is an optically thick line, its peak intensity is proportional to the $2/[3(1 + \gamma)] = \frac{4}{9}$ power of optical depth (Panagia 1988). Therefore, the condition that the intensity contributed by the sub-$v_0$ layers, i.e., between $R_*$ and $R_0$, be lower than the detection limit of 4%, i.e., $I_* \le 1.04 \times I_0$, can be written as

$$\tau_* \le (1.04)^{9/4}\tau_0 , \tag{2}$$

where $\tau_*$ is the optical depth from the stellar photosphere to infinity and $\tau_0$ the one from $R_0$ to infinity. Adopting an average density $\bar{n} = (v_0/v_{sound})^{1/2}n(R_0)$ for the region between $R_*$ and $R_0$, and defining $\Delta R = R_0 - R_*$, after simple algebra equation (2) gives the following inequality

$$\Delta R/R_0 \le 0.016 , \tag{3}$$

This indicates that our initial radius $R_0$ may be only marginally larger than the true photospheric radius. Therefore, in the following we shall adopt the photospheric radius as the value of initial radius of the wind. From this argument it is also clear

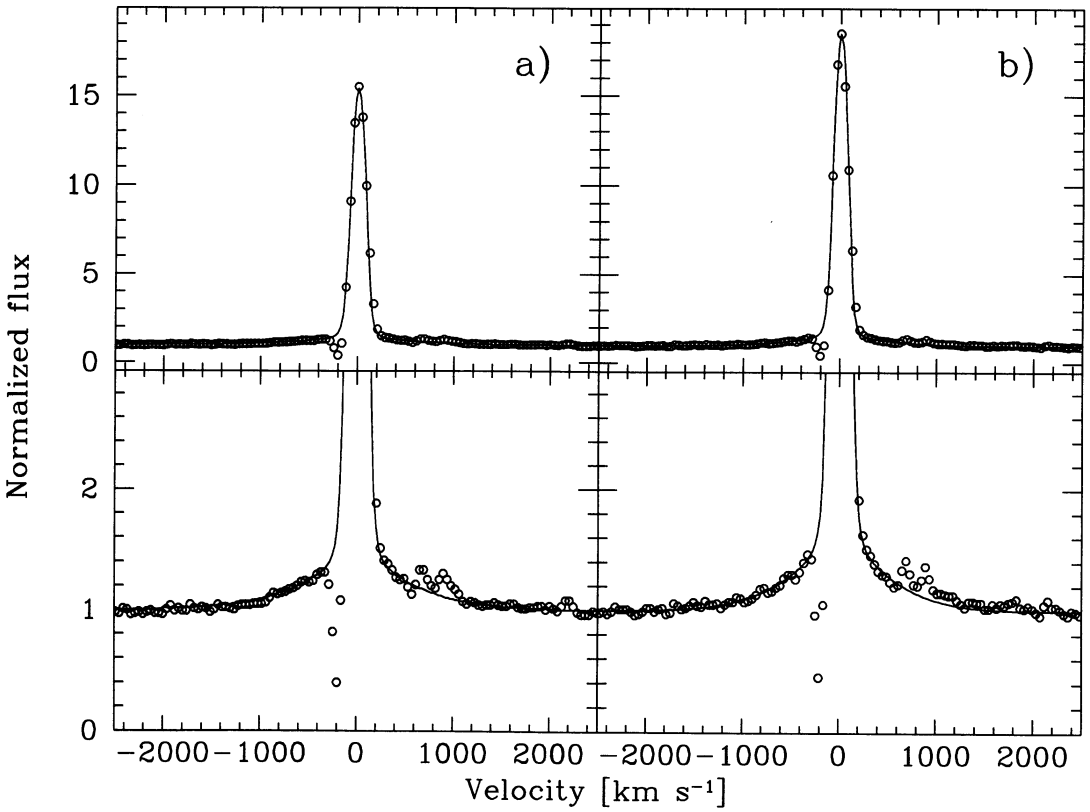


FIG. 3.—Two examples of fit of the Hα line profile: the dots are the observations and the solid line is the theoretical profile. Fig. 3*a* refers to the line observed on 1989 October 5, while Fig. 3*b* to the line observed on 1991 July 23.

that the wind must undergo a fast acceleration just above the stellar photosphere (about 30 km $s^{-1}$ in little more than 1 $R_\odot$) whereas, past $R_0$, the push becomes much more gentle.

The line radiation transfer is treated adopting the Sobolev approximation. The line profile results from the combination of photospheric absorption with emission and resonant scattering in the wind (see Scuderi et al. 1992 for a detailed description of the profile calculation). The photospheric profile, deduced from the grid of model atmospheres computed by Mihalas (1972), has been rotation broadened adopting a rotational velocity for P Cyg, $v \sin i$, of 75 km $s^{-1}$ (Hoffleit & Jaschek 1982).

The calculated profiles reproduce the cores of the observed lines quite well but do not match the Hα wing profiles closely enough, as already noticed in Scuderi et al. (1992). In particular, the observed profiles display a blue absorption and broad emission wings not reproduced by the model.

The failure in reproducing the blue absorption is to be ascribed to the method of the line profile calculation for the following reason. The underlying photospheric absorption profile does not produce a significant absorption at velocities where the observed absorption occurs ($\sim -150$ km $s^{-1}$). As the isothermal wind produces only emission, the emerging profile at $\sim -150$ km $s^{-1}$ is completely in emission. The presence of the absorption component in the blue wing shows that the source function in the wind drops at a distance of about 7 $R_*$, where $v \sim -150$ km $s^{-1}$. However, the relative contribution of the absorption component to the total equivalent width of Hα is about two orders of magnitude smaller than that of the emission component, which, in turn, is well matched by our model calculations. Therefore, it is clear that the determination of the mass-loss rate is unaffected by the inadequate fit of the absorption component.

The broad-line wings can be attributed to Thomson scattering by free electrons in the formation region of the Hα line, as already suggested by Bernat & Lambert (1978). To include this effect we proceed as follows.

We consider a case in which emitters (protons recombining with electrons) and scatterers (free electrons) are intimately mixed. The intrinsic input profile of the line radiation is the one calculated by our model. The profile that emerges after interaction with the free electrons is given by

$$I(x) = \epsilon\phi(x) + (1 - \epsilon)\int_{-\infty}^{+\infty} \phi(x')R(x, x')dx' , \qquad (4)$$

where $x$ and $x'$ are observed velocities (expressed in units of the electron thermal velocity); $\phi(x)$ is the incident line profile; $R(x, x')$ is the electron scattering redistribution function (Mihalas 1970); and $\epsilon$ is the fraction of nonscattered radiation, given by

$$\epsilon(\tau_e) = \frac{1 - e^{-\tau_e}}{\tau_e} , \qquad (5)$$

where $\tau_e$ is the electron scattering optical depth. In our model, $\tau_e$ can be expressed in terms of stellar and wind parameters as

$$\tau_e = \frac{n_{e0}\,\sigma_e\,R_0}{1 + \gamma} , \qquad (6)$$

where $n_{e0}$ is the electron density at the base of the wind, $\sigma_e$ is the Thomson scattering cross section, $\gamma$ is the exponent of the velocity power law, and $R_0$ is the lower boundary of the line-emitting region.

With respect to the line profile fit described in Scuderi et al. (1992), we have now two additional free parameters for the model fit to the observations. These new parameters are the electron scattering optical depth, $\tau_e$, and the kinetic temperature of the free electrons, $T_e$, which add to the other three fit parameters, i.e., the optical depth in the Hα line, $\tau_0$, the initial velocity of the wind at the base of the wind, $v_0$, and the exponent $\gamma$ of the velocity power law.

To fit the Hα profile we proceed as follows.

1. We assume a value for the exponent $\gamma$.
2. We estimate $\tau_0$ and $v_0$ from a fit of the observed line core.
3. With these parameters we compute the incident profile $\phi(x)$.
4. By means of equation (1) we obtain $I(x)$ varying $T_e$ and $\tau_e$ until a satisfactory fit is obtained.

The above procedure is iterated until convergence is achieved. The whole process is repeated for different values of $\gamma$, and the final values of the parameters are identified with a minimum $\chi^2$ test applied to the fit of the whole profile.

The best fits of two Hα line profiles are shown in Figure 3. We see that the model reproduces the observed profiles quite well, in both the emission component of the line and the broad emission wings, whereas the agreement between models and observations for the blue absorption component is not perfect.

## 4. RESULTS

The fit of the Hα profile allows us to describe the properties of the wind, i.e., the electron temperature, the velocity field of the wind, and the mass-loss rate in terms of $v_0$, $\gamma$, $T_e$, $\tau_0$, and $\tau_e$. The values of these parameters, except $T_e$, are reported in Table 1 for the various observing epochs.

### 4.1. *The Electron Temperature*

The fitting procedure showed that the wings of the Hα line are not very sensitive to the electron temperature. We have estimated the a priori accuracy of an individual determination of $T_e$ to be about 30%. Therefore, this quantity cannot be determined accurately from line profile fitting. We have calculated the root mean square deviation of the $T_e$ values obtained from line fitting and we have found it to be $\pm 14\%$ of the average $T_e$. This means, first of all, that our a priori estimate of the $T_e$ error was pessimistic, and second, that the variations we see, being of the same order as the expected error, may entirely be due to errors. Thus, we only say that, *if* there are variations, they must be smaller than 14%.

For the calculation of the mass-loss rate we adopted the average of the values found from the line profile fit, i.e., $T_e =$ 13,000 K, which corresponds to about 70% of the effective temperature ($T_{\rm eff}$ = 19,300 K; Lamers et al. 1983).

### 4.2. *The Velocity Field*

The velocity field of the wind of P Cyg appears to be variable. The velocity law exponent $\gamma$ was always found to be 0.5 with a possible uncertainty of $\pm 10\%$. The initial wind velocity $v_0$ shows irregular variations of up to 20% (Fig. 4), which seem to be real. This conclusion is supported by the fact that the variations of $v_0$ are anticorrelated with those of $\tau_0$ (see Fig. 5), i.e., with the variations of the strength of the Hα line.

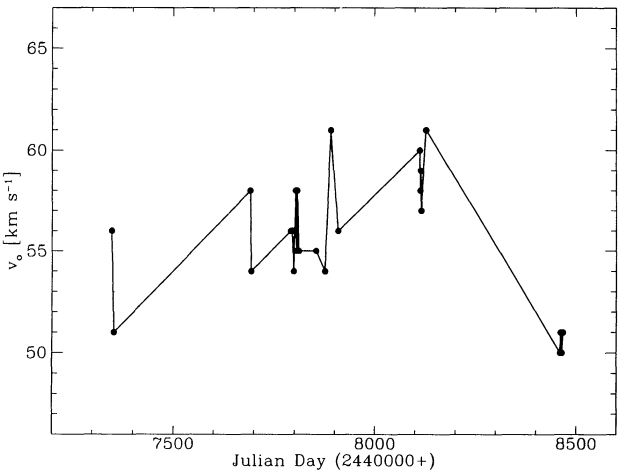


FIG. 4.—The initial velocity as a function of time

The value of the exponent $\gamma$ agrees quite well with the findings of Felli et al. (1985), who estimated $\gamma = 0.7 \pm 0.3$ from an analysis of the recombination lines and the continuum in the near-infrared.

The values of the initial velocity are about 3 times larger than the sound speed in the stellar atmosphere ($\sim$19 km s$^{-1}$). This means that the wind material undergoes a fast initial acceleration from the sound speed to the observed initial velocity near $r = R_0$. Past that point, the velocity increases very gradually with a shallow gradient, approaching its terminal value at more than 15 stellar radii. This behavior agrees with the results obtained by Pauldrach & Puls (1990) by model fitting the UV and the IR spectrum of P Cyg.

### 4.3. *Determination of the Mass-Loss Rate*

The mass-loss rate can be evaluated from the fitting parameters in two independent ways, i.e., from the optical depth of the Hα line and from the optical depth for electron scattering. Since the former is proportional to the square of the density whereas the latter depends linearly on the density, a compari-

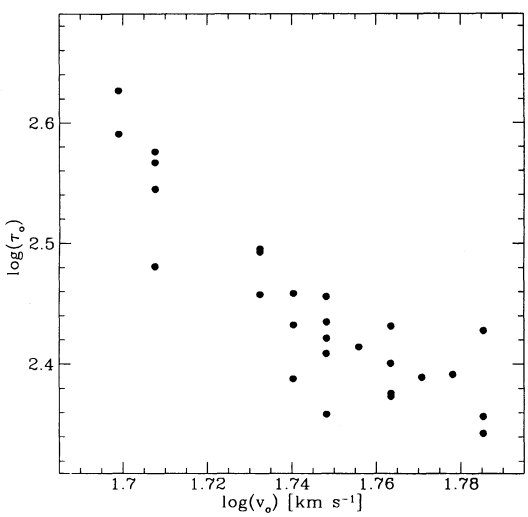


FIG. 5.—The correlation of the initial velocity with the Hα optical depth

son of the two determinations will provide an estimate of the importance of clumping in the wind.

As we said, a first method to determine the mass-loss rate is based on the computation of the Hα optical depth, $\tau_0$, which is related to the mass-loss rate by the equation (Scuderi et al. 1992):

$$\dot{M} = 0.203\mu_e\left[1 + \frac{n(\mathrm{He}^+)}{n(\mathrm{H}^+)}\right]^{1/2}\left(\frac{\tau_0}{b_2}\right)^{1/2} \times \left[\frac{T_e}{10^4\ \mathrm{K}}\right]^{3/4}\left[\frac{R_0}{10\ R_\odot}\right]^{3/2}\left[\frac{v_0}{100\ \mathrm{km\ s^{-1}}}\right]^{3/2} \times (e^{E_2/kT} - e^{E_3 - kT})^{-1/2} 10^{-6}\ M_\odot\ \mathrm{yr}^{-1}\ , \quad (7)$$

where $\mu_e$ is the mean atomic weight per electron, given by

$$\mu_e = \frac{\sum_i X_i m_i}{\sum Z_i M_i}\ , \quad (8)$$

$X_i$, $m_i$ and $Z_i$ are, respectively, the abundance by number, mass, and charge of the $i$th ion; $E_2$ and $E_3$ are respectively the ionization energies from the second and the third level; $b_2$ is the ratio of the population of the second level to that in LTE, and we have also explicated the dependence on helium abundance with respect to hydrogen. This method will henceforth be referred to as the $\tau_0$ method.

On the other hand, taking into account the electron scattering allows not only a fit of the broad wings of the Hα line but also provides a second, independent method to estimate the mass-loss rate of the star. The determination of the electron scattering optical depth, $\tau_e$, which is related to the mass-loss rate by equation (6):

$$\dot{M} = 3.45\mu_e\tau_{e*}(1+\gamma)\left[\frac{v_0}{100\ \mathrm{km\ s^{-1}}}\right]\left[\frac{R_0}{10\ R_\odot}\right]10^{-6}\ M_\odot\ \mathrm{yr}^{-1}\ . \quad (9)$$

We will refer to this method as to the $\tau_e$ method. To compute $\dot{M}$ from equations (7) and (9) we use the values of $\gamma$, $v_0$, $\tau_0$, $\tau_e$ deduced from the line fit. We adopted an abundance of $n(\mathrm{He}^+)/n(\mathrm{H}^+) = 0.5$ (Barlow 1991), and $\mu_e = 2.0$, as we have assumed the gas to be composed of ionized hydrogen and singly ionized helium only. A high He abundance, which was inferred by Barlow on the basis of near-IR lines, is confirmed by the ratio $W$(He I 6678)/$W$(Hα). Our observations give an average value of 0.057 which corresponds to $n(\mathrm{He}^+)/n(\mathrm{H}^+) = 0.48$ if the two lines are interpreted in terms of an optically thin layer in the case B approximation.

For the population of the $n = 2$ and $n = 3$ levels of H we adopted $b_2 = b_3 = 1.3$ suggested by the non–LTE calculations of the winds of O stars by Klein & Castor (1978). Values of this order were determined by Felli et al. (1985) from a model fitting of near-IR line intensities ($b_4 \sim 3$, $b_5 \sim 2$, $b_7 \sim 1.4$ for $\gamma \sim 0.5$). In any case, it must be understood that these are merely average values in the line-forming region of the wind. A non–LTE wind model calculated by one of us (A. d. K.) shows that actually the departure coefficients $b_3$ and $b_2$ are not constant in the wind, but vary between extreme values form about 1 to 10. Therefore, the adopted constant values of $b_2$ and $b_3$ may be uncertain by as much a factor of 2.

The other two physical parameters to determine are the electron temperature, $T_e$, and the stellar radius, $R_*$. With regard to the electron temperature we have already mentioned (see § 4.1) that the line fit allows us to determine only a mean value of $T_e$. Furthermore, the line fit does not give any information about the radius.

Therefore, we have first calculated $\dot{M}$ assuming $T_e$ and $R_0$ to be constant and equal to 13,000 K (see § 4.1) and to 76 $R_\odot$, respectively. We have done this to check the consistency of the $\tau_0$ method and the $\tau_e$ method for the estimate of the mass-loss rate and also to determine which one gives the best estimate of $\dot{M}$.

The results of these calculations are shown in Figure 6. It is clear that the two mass-loss rate determinations agree quite well with each other. We also note that, although both methods are able to provide a good estimate of the mass-loss rate, the $\tau_0$ method, while intrinsically more precise, may be affected by larger uncertainties because of the uncertainty of the assumed values of $b_2$ and $b_3$. As a consequence, the *absolute value* of $\dot{M}$ is in principle more reliably determined with the $\tau_e$ method whereas the time variations are better determined with the $\tau_0$ method. In practice, in the following we will conclude that our choice of the $b$-factors is quite adequate for the case of P Cyg, at least, and that, therefore, the $\tau_0$ method can reliably be used in most cases.

We note that the good agreement of the mass loss determined with the two independent methods, which are sensitive to $n_e^2$ and $n_e$, respectively, implies that clumping in the wind is not important.

The plot of the mass-loss rates data versus time (Fig. 7) shows that, keeping $R_0$ and $T_e$ constant, the mass-loss rate fluctuates around a mean value of about $1.9 \times 10^{-5}\ M_\odot\ \mathrm{yr}^{-1}$ with no clear systematics. The precision of an $\dot{M}$ determination depends on quantities which are directly observed: the equivalent width and the half-power full width. It also depends on assumed quantities: the value of the non–LTE parameters $b_2$ and $b_3$ and on the radius and the effective temperature of the star. As these last two quantities are not known very precisely (the relative errors are 18% for $R$ [Lamers et al. 1983] and 14% for $T_e$ [see § 4.1]) the a priori uncertainty on individual determinations of the *absolute* value of $\dot{M}$ is estimated to be 39%.

Our estimate of the average mass-loss rate of P Cyg compares very well with determinations obtained from both IR

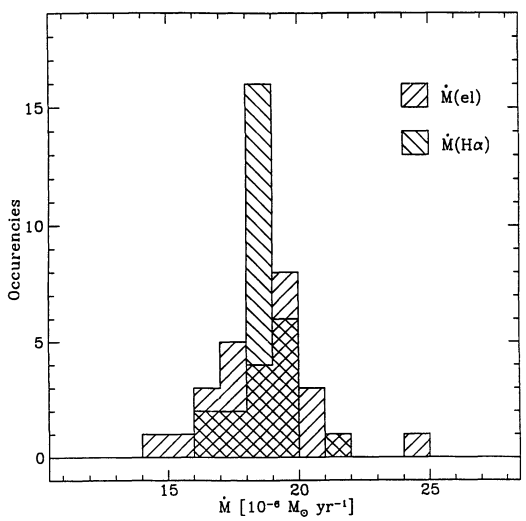


FIG. 6.—Comparison of the mass-loss rate obtained from the Hα optical depth with that obtained from the electron scattering optical depth.

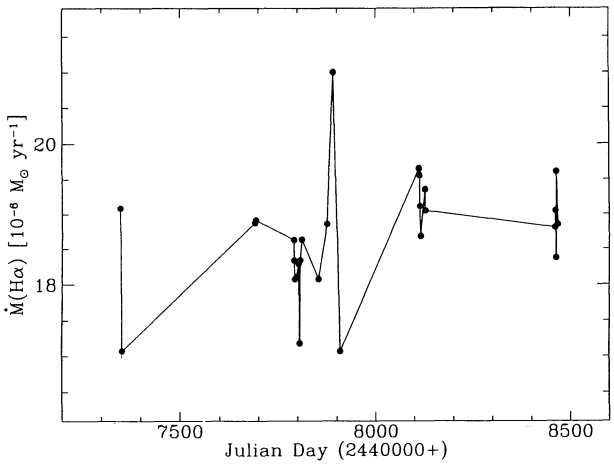


FIG. 7.—The temporal behavior of the mass-loss rate obtained from the Hα optical depth assuming $R$ and $T_{\rm eff}$ to be constant.

and radio observations. In fact, the results of Felli et al. (1985) give $\dot{M}_{\rm IR} = (2.2 \pm 0.7) \times 10^{-5}\ M_\odot\ {\rm yr}^{-1}$ after readjusting the He abundance and the initial wind parameters to our values. Also, using the results of Pauldrach & Puls (1990) analysis of the available radio data and, again with a readjustment for the He abundance, the mass-loss rate turns out to be $\dot{M}_{\rm radio} = (1.5 \pm 0.5) \times 10^{-5}\ M_\odot\ {\rm yr}^{-1}$ if a terminal velocity of 200 km s$^{-1}$ (Lamers et al. 1985) is adopted. These results suggest that the uncertainty in the $b$ factors is likely to be considerably less than a factor of 2.

Combining the three independent determinations we obtain a rather accurate value for the P Cyg mass-loss rate of $\dot{M} = (1.87 \pm 0.35) \times 10^{-5}\ M_\odot\ {\rm yr}^{-1}$.

### 4.4. *Analysis of the Variability of P Cygni*

If we are interested only in the study of the mass-loss variations, we have to exclude from the computation of the error on $\dot{M}$ all the contributions which affect only its absolute value. In this case, we have to exclude the errors on $T_e$ and $R$. Thus, the estimated uncertainty in $\dot{M}$ variations is about 7%. The fluctuations seen in Figure 7 are of the same order as the expected error and, therefore, are likely not to be significant. Therefore, it appears that during the 4 yr covered by our spectroscopic observations the mass-loss rate has not varied appreciably.

We still have to consider the effect of the $R_*$ and $T_e$ variations on $\dot{M}$. The time variations of the effective temperature, $T_{\rm eff}$, and the radius, $R$, can be estimated from photometric data. However, since the absolute values obtained from the analysis of these data are rather uncertain we determined only the relative variations of the two parameters.

#### 4.4.1. *$T_e$ Variations from Photometric Data*

We do not have a direct means to measure the variations of the electron temperature. If we assume that the electron temperature in the wind is proportional to the effective temperature of the star, the relative variations of $T_e$ are equal to those of the effective temperature which can be obtained from the photometric data.

Relative variations in the effective temperature were estimated separately from the observed $U-B$ and $B-V$ color indices. We corrected them for insterstellar extinction, adopting $E(B-V) = 0.63$ (Lamers et al. 1983), and we calculated $T_{\rm eff}$ by using the compilation of the intrinsic colors $(B-V)_0$ and $(U-B)_0$ versus $T_{\rm eff}$, given by Schmidt-Kaler (1982).

The results plotted in Figure 8*c*, for the $B-V$ color index, and in Figure 9*c*, for the $U-B$ color index, show irregular variations superposed on a systematic decrease. The errors on the observed colors limit the determination of the relative variations $\Delta T_{\rm eff}/T_{\rm eff}$ to within about 3%, and this means that both the irregular and the systematic observed variations are significant.

#### 4.4.2. *$R_*$ Variations from Photometric Data*

Once the effective temperature is known, the angular diameter of the star can be calculated from the visual magnitude using the formula (Schmidt-Kaler 1982)

$$\log \theta = -2 \log (T_{\rm eff}) - 0.2\ {\rm BC} - 0.2(m_V - A_V) + 8.442\ , \quad (10)$$

where $\theta$ is the diameter of the star ($2R/d$), BC is the bolometric correction computed by means of a relationship BC versus $T_{\rm eff}$ (Schmidt-Kaler 1982), $m_V$ is the apparent magnitude in the $V$ band, and $A_V = 3.1 \times 0.63 = 1.95$. In adopting the relation between BC and $T_{\rm eff}$ from normal supergiants, we assumed implicitly that the star remains in thermal equilibrium during the variations. If the variations are due to pulsations this assumption may not be fully verified.

Figures 8*b* and 9*b* show $\Delta R/R$ versus time as deduced from the $B-V$ and $U-B$ color indices measurements, respectively. Again we see irregular variations superposed, this time, on a systematic increase. The precision of the $\Delta R/R$ estimates is about 2%, which tells us that the observed variations are real.

The $R$ and $T_{\rm eff}$ variations are clearly anticorrelated, indicating that the luminosity of P Cygni remains constant during the photometric variations.

#### 4.4.3. *Mass-Loss Rate*

As mentioned in § 2.2, the spectroscopic and the photometric observations were not always simultaneous. Therefore, for some epochs the value of $R$ and $T_e$ had to be interpolated

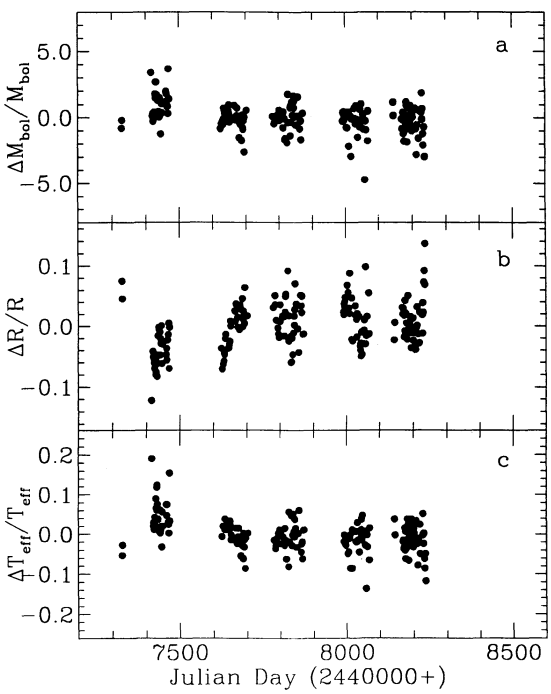


FIG. 8.—Relative variations of (*a*) the bolometric magnitude, (*b*) the radius, and (*c*) the effective temperature as obtained from the $B-V$ color indexes.

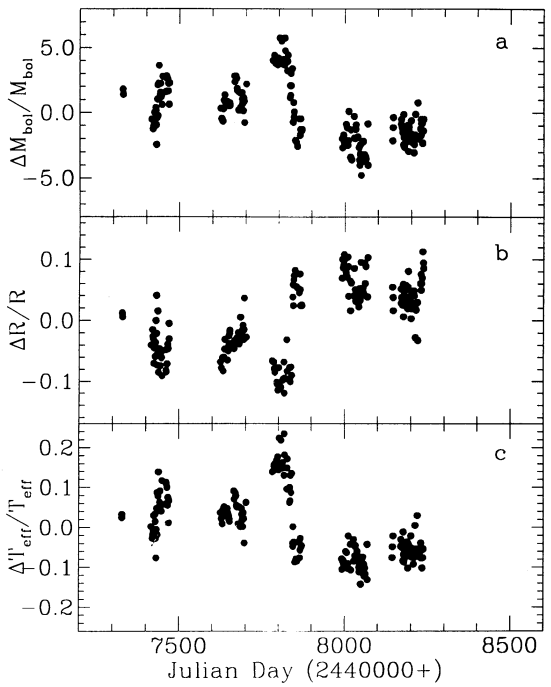


FIG. 9.—Relative variations of (*a*) the bolometric magnitude, (*b*) the radius, and (*c*) the effective temperature as obtained from the $U-B$ color indexes.

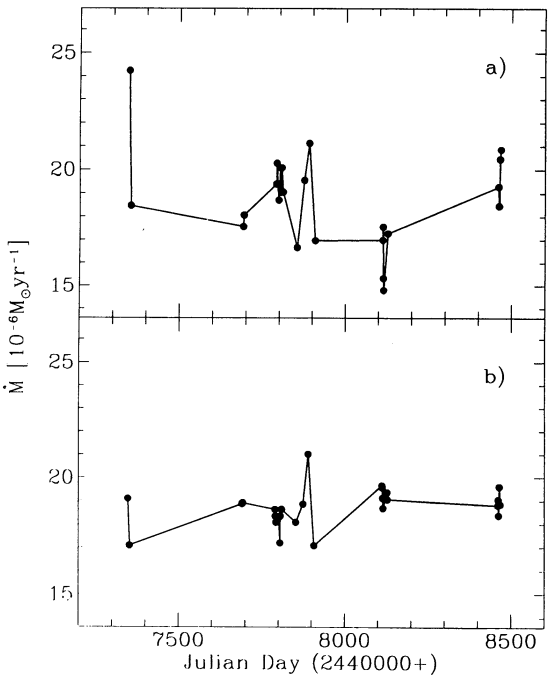


FIG. 10.—The mass-loss rate obtained taking into account the $T_{eff}$ and $R$ variations as obtained from (*a*) the $U-B$ color indexes and (*b*) the $B-V$ color indexes.

among the available values. The stellar radius and the electron temperature for each of the observing epochs were calculated relative to the adopted reference values of $R_*$ and $T_e$, i.e., $R_* = 76R_\odot$ and $T_e = 13{,}000$ K.

The mass-loss rates obtained using the $\tau_0$ method, but correcting for the variations in the electron temperature and the stellar radius deduced from $B-V$ measurements, are shown in Figure 10*a*. They show a temporal behavior similar to that of Figure 7, which was obtained keeping $R$ and $T_e$ constant. The results are somewhat less reliable for epochs at which simultaneous photometric and spectroscopic data were not available, so the photometric measurements had to be either interpolated (1990 August) or even extrapolated (1991 July). At any rate, the overall behavior of the mass-loss rates is the same: one sees no systematic trend but only irregular variations of 10% around a mean value of about $1.9 \times 10^{-5}\ M_\odot\ yr^{-1}$. In the error calculation we have included the errors in the variations of $R_*$ and $T_e$. These irregular variations in $\dot{M}$ are not likely to be significant because they have an amplitude comparable to the observational uncertainties. On the other hand, if they were real, they might be accounted for by the ejection of suitable shells, similar to those revealed by the analysis of UV line profile variations (Cassatella et al. 1979; Lamers 1987) if their mass is about $M_{shell} \simeq 10^{-8}\ M_\odot$ (see Appendix). In any case, their contribution to both the Hα line intensity and to the mass loss would remain of marginal importance. We conclude that the variations in $R$ and $T_e$ compensate each other yielding a mass-loss rate practically constant to within ±10% (rms) throughout the period covered by the observations. In other words, the apparent variations of the Hα equivalent width are mostly due to variations of the stellar continuum rather than to intrinsic changes of the mass-loss rate.

The mass-loss rates obtained using $\Delta R$ and $\Delta T_e$ as deduced from $U-B$ measurements are plotted as a function of time in Figure 10*b*. These results do not agree quite well with those derived from $B-V$ photometry. The most striking difference is the jump in the mass-loss rate around JD 2,447,800. In an attempt to understand the cause of this increase, we examined the photometric data in the corresponding period and found that around that time the $U-B$ color shows a relative dip which lasts about 50 days. Since neither the $B$ nor the $V$ magnitude show a similar behavior, we argue that these variations are entirely due to $U$-band variations. Just on the basis of pure photometry it is hard to assess whether these $U$-band variations reflect changes in the radiation flux and/or the structure of the photosphere or that they are merely the result of relatively modest changes that effect absorption/emission features in the spectrum around 3600 Å. In the absence of additional information we regard these variations as not relevant for our analysis and will not discuss this point any further in this paper.

### 4.5. *Luminosity Variations*

The photometric data were also used to study the luminosity variations in P Cyg. Figures 8 and 9 show the relative variations of the bolometric magnitude as obtained from $B-V$ (Fig. 8*a*) and $U-B$ (Fig. 9*a*) data. An inspection of these plots shows that the luminosity has not changed systematically but has just fluctuated around a mean value. Actually, the $U-B$ data show a rapid variation around the observational period we mentioned above, but which may not be significant. The precision of the $\Delta M_{bol}/M_{bol}$ *relative* variations obtained from $B-V$ photometry is about 8% and 5% from the $U-B$ photometry.

### 4.6. *Correlation between Stellar Parameters and Wind Properties*

The results outlined in the previous paragraphs give some insight in the way the stellar parameters and the physical quantities which characterize the wind are related.

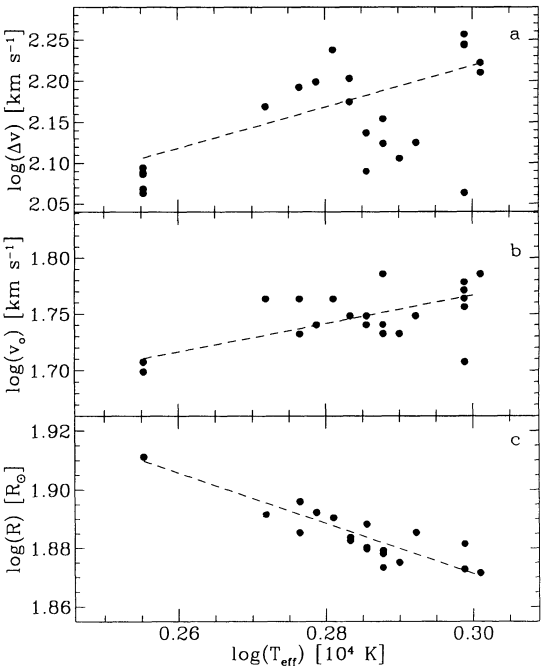


FIG. 11.—Correlations of $T_{\rm eff}$ with $R$, and with two physical quantities characteristic of the wind velocity field, $v_0$ and $\Delta v$ (see text for explanation).

First of all, it is interesting to note that both the mass-loss rate and the luminosity are found to remain constant over the whole period of observations while the stellar radius and effective temperature, as well as the initial velocity of the wind and the Hα optical depth (hence the average density in the wind), display significant variations. These results are easily understood in a scheme in which the mass loss is entirely determined by the energy output of a star, whereas the detailed wind characteristics (velocity and/or density) depend on the "quality" of the radiation field through the effect of radiation pressure by resonance lines, according to an early suggestion made by Panagia & Macchetto (1982).

Within this scenario one should expect some sort of correlation among the stellar parameters which influence the UV flux and then the acceleration of the wind, and the physical parameters which characterize the wind velocity field. Since $T_{\rm eff}$ and $R$ are clearly correlated with each other (Fig. 11*c*), we looked only for possible correlations of the wind parameters with the effective temperature. As characteristic parameters of the velocity field we took the initial wind velocity $v_0$ and, since we cannot measure the terminal velocity from the Hα profile, the position of the minimum absorption $\Delta v$, calculated with respect to the emission peak position. The results of this analysis are presented in Figure 11*b* and 11*a*. There is evidence for a weak but a clear correlation in the sense that higher temperatures correspond to greater velocities. The straight lines are best-fit lines of the data. Although the scatter of the points is rather high due to the observational errors (about 10%, 14%, and 3% for $v_0$, $\Delta v$, and $T_{\rm eff}$, respectively), these correlations are significant because we find correlation coefficients of 0.7 and 0.5 for the $v_0$ and $\Delta v$ regressions, respectively.

## 5. CONCLUSIONS

A program of spectroscopic observations of P Cyg in the Hα region has been carried out at the Catania Astrophysical Observatory in order to study the properties and the time variability of the stellar wind. The results obtained from the analysis of the data collected in the period 1988 June–1991 July were presented here. In addition, we used *UBV* photometric data to have information on the temporal variations of the radius and the effective temperature of P Cyg.

By using the model described in Scuderi et al. (1992) and further improved to include the effect of scattering by free electrons, we calculated theoretical Hα profiles to fit the observed ones. The profile fit allowed us to determine the temporal behavior of the wind properties. The results can be summarized as follows.

1. The average electron temperature in the wind is (13,000 ± 1800) K (the error is the rms of the $T_e$ values). Since the accuracy of individual determinations is of the same order as the expected error, the temperature variations must be smaller than 15%.

2. The mass-loss rate remained constant to within ±10% (rms) over the 3 yr period covered by our observations (1988 June through 1991 July). Our mass-loss determinations give a mean rate of $(1.9 \pm 0.2) \times 10^{-5}\ M_\odot\ {\rm yr}^{-1}$ where the error represents the standard deviation of the mass-loss determinations over the period covered by the observations. The mean mass-loss rate agrees quite well with independent determinations based on IR and radio data. This confirms the accuracy of our method also for a determination of the mass-loss rate *absolute value* in addition to its variations.

3. In the same period the bolometric luminosity also stayed constant to within ±10%.

4. The velocity field, and therefore the electron density of the wind, were found to be variable. In particular, the initial wind velocity, $v_0$, shows irregular variations which we found to be correlated with the strength of the Hα line.

5. These results, together with the constancy of the stellar luminosity over the period of observations, suggest that while the "shape" of the spectrum emitted from the star determines the kinematic properties of the wind, the mass-loss rate is entirely determined by the total luminosity of the star.

6. Our data show that possible effects of clumping of the wind material and/or ejection of discrete shells are negligible.

S. S. acknowledges the hospitality of the Space Telescope Science Institute where part of this work has been done. We wish to thank Rita Ventura for kindly providing the code for the periodicity analysis.

## APPENDIX

## EFFECTS OF DISCRETE SHELL EJECTION ON THE MASS LOSS

There are two kinds of shells which have been identified from the study of UV and optical line profiles of P Cyg (Lamers 1987; Cassatella et al. 1979): one which gives rise to variable components in the profile; has a velocity ranging from $-50$ km s$^{-1}$ to $-150$ km s$^{-1}$, a lifetime of about 1 yr and a column density of $N_{\rm H} \simeq 10^{18}$ cm$^{-2}$, and a stable component which produces a steady

absorption at a velocity of $v \simeq 200$ km s$^{-1}$; and has a column density $N_H \simeq 10^{20}$ cm$^{-2}$. The mass of the latter is about $3 \times 10^{-7}$ $M_\odot$ while the former has a much lower mass, say, about $3 \times 10^{-11}$ $M_\odot$. It is immediately clear that the known phenomenon of shell ejection can hardly affect the average mass-loss rate. In fact, even the ejection of a massive shell per year (which below we argue is very unlikely to occur) would correspond to a change of the average mass-loss rate of a few percent.

As for H$\alpha$ line intensity, let us address the problem of whether the observed variability in the H$\alpha$ equivalent width may be due to the ejection of discrete shells. First we consider the ones that produce variable absorption components in UV line profiles. The calculations have been made assuming a shell to be uniform, to have a radius $r = 10R_*$ (which corresponds to $-150$ km s$^{-1}$ in P Cyg's velocity field), and with $\Delta r$ = *thickness of the shell* $= 0.1r$:

$$N_H = n_e \Delta r = 10^{18} \text{ cm}^{-2}, \quad r = 10R_* = 5.3 \times 10^{13} \text{ cm}, \quad \Delta r = 5.3 \times 10^{12} \text{ cm}, \quad n_e = 1.9 \times 10^5 \text{ cm}^{-3},$$

$$L(\text{H}\alpha) = h\nu_{\text{H}\alpha}\, \alpha_{\text{H}\alpha}\, n_e^2 4\pi r^2 \Delta r = 1.5 \times 10^{27} \text{ ergs s}^{-1},$$

where $\alpha_{\text{H}\alpha} = 7.7 \times 10^{-13}$ cm$^3$ s$^{-1}$ is the effective recombination rate for the H$\alpha$ line at a temperature of 13,000 K (Spitzer, 1978, p. 89) and $L$(H$\alpha$) is the H$\alpha$ luminosity produced by a shell, assumed to be optically thin, which is the most favorable hypothesis. The luminosity of the continuum at the H$\alpha$ wavelength, which has been estimated from $M_V$ and from Kurucz model atmospheres, is $\sim 4.9 \times 10^{34}$ ergs s$^{-1}$ Å$^{-1}$ and, therefore, the contribution to the H$\alpha$ equivalent width is

$$W_{\text{transient shell}} \simeq 3.2 \times 10^{-8} \text{ Å},$$

which is absolutely negligible.

Even if we shrink the shell to a size equal to the stellar radius, so as to simulate its insurgence from the photosphere, the emission remains quite small. In fact, keeping the shell mass constant and assuming homologous expansion, its emission scales like $r^{-3}$ and, therefore. we have

$$W(r = R_*)_{\text{transient shell}} \simeq 3.2 \times 10^{-5} \text{ Å},$$

which is still negligible. Therefore, this kind of shell cannot account for any appreciable fraction of the H$\alpha$ emission from P Cyg, nor for any detectable variations.

For the stable component we can repeat the same kind of analysis. Assuming a typical radius for the shell of $100R_*$ (Lamers 1989) we obtain

$$W_{\text{stable shell}} \simeq 3.2 \times 10^{-3} \text{ Å}$$

which is also quite small. Therefore, it is clear that none of the discrete shells *actually detected* from studies of UV line profiles can be of any importance for the emission of H$\alpha$ radiation in the period covered by our observations.

However, it is interesting to note that a shell of ionized gas, with a mass equal to that of the stable component and a radius equal to the stellar radius, would produce a very strong H$\alpha$ emission, say, an order of magnitude higher, or even more, than the observed line intensity. This fact suggests that the "stable" shell may not be the result of a single ejection event but rather consists of material that has been accumulating over a relatively long time. If, on the other hand, the ejection of such thick shells is indeed possible, then our observations indicate that no such event has taken place over the 3 yr we monitored P Cyg.

Moreover, we can use the same line of arguments to estimate that a shell with a mass of about $10^{-8}$ $M_\odot$ and initial column density $N_H(r = R_*) \simeq 3 \times 10^{22}$ atoms cm$^{-2}$ would be able to increase the equivalent width of H$\alpha$ by several angstroms and, therefore, could account for the possible fluctuations of the H$\alpha$ intensity. Since the emission of a shell decreases like $r^{-3}$ and the expansion velocity is about 100 km s$^{-1}$, the shell emission would decay by a factor of 2 in a time of $\sim 2^{1/3} R_*/v_{\text{exp}} \simeq 8$ days, which indeed is comparable to the timescale of fluctuations. Therefore, it is possible that the ejection of suitable discrete shells account for the observed fluctuations. Note that the shell column density corresponds to an optical depth for Thomson scattering of less than 0.02 which indicates that the ejection of one such shell does not affect the stellar continuum.

One may go a step further and ask if the *whole* mass loss may consist of discrete shells. If this were the case, one would need the ejection of about $\dot{M}/M_{\text{shell}} = 1.9 \times 10^{-5}$ $M_\odot$ yr$^{-1}$/$10^{-8}$ $M_\odot$ = 1900 shells per year, i.e., about 5 per day. This number is so high that the average time between the ejection of successive shells is much shorter than the decay time of the emission of an individual shell. As a consequence, only fluctuations of less than 1% may be expected and, therefore, the phenomenon would not be distinguishable from that of a steady mass loss.

In summary, we conclude the following.

1. During the period covered by our observations, the emission of H$\alpha$ line radiation from P Cyg may entirely be accounted for by a steady, uniform wind. The H$\alpha$ emission from discrete shells can represent but a very minor contribution to the observed value.
2. In particular, the type of shells that characterize the variable components detected in the profiles of UV lines produce an H$\alpha$ emission which is several orders of magnitude lower than the observed line strength.
3. The ejection of shells with mass $M_{\text{shell}} \simeq 10^{-8}$ $M_\odot$ may account for the fluctuations of the H$\alpha$ intensity at a few percent level.
4. No discrete shell with mass greater than $\sim 10^{-8}$ $M_\odot$ has been ejected during the period covered by our observations.

REFERENCES

Abbott, D. C., Bieging, J. H., & Churchwell, E. 1981, ApJ, 250, 645
Barlow, M. J. 1991, in IAU Symp. 143, Wolf-Rayet Stars and Interrelations with Other Massive Stars in Galaxies, 281
Barlow, M. J., & Cohen, M. 1977, ApJ, 213, 737
Bernat, A. P., & Lambert, D. L. 1978, PASP, 90, 520
Cassatella, A., et al. 1979, A&A, 79, 223
de Groot, M. 1969, BAN, 20, 225
Ebbets, D. 1982, ApJS, 48, 399
Felli, M., & Panagia, N. 1981, A&A, 102, 424
Felli, M., Stanga, R. Oliva, E., & Panagia, N. 1985, A&A, 151, 27
Gathier, R., Lamers, H. J. G. L. M., & Snow, T. P. 1981, ApJ, 247, 17
Hoffleit, D., & Jaschek, C. 1982, The Bright Star Catalogue (New Haven: Yale University Observatory)
Klein, R. I., & Castor, J. I. 1978, ApJ, 220, 902
Lamers, H. J. G. L. M. 1987, in Instabilities in Luminous Early-Type Stars, ed. H. J. G. L. M. Lamers & C. W. H. de Loore (Dordrecht: Reidel), 99
———. 1989, in Physics of Luminous Blue Variables, ed. K. Davidson, A. F. J. Moffat, & H. J. G. L. M. Lamers (Dordrecht: Kluwer), 135
Lamers, H. J. G. L. M., de Groot, M., & Cassatella, A. 1983, A&A, 128, 299
Lamers, H. J. G. L. M., & de Groot, M. 1992, A&A, 257, 153
Lamers, H. J. G. L. M., & Fitzpatrick, E. 1988, ApJ, 324, 279
Lamers, H. J. G. L. M., Korevaar, P., & Cassatella, A. 1985, A&A, 149, 29
Leitherer, C. 1988, ApJ, 326, 356
Mihalas, D. 1970, in Stellar Atmospheres (San Francisco: Freeman), 321
———. 1972, NCAR-TN/STR-76
Panagia, N. 1988, in Galactic and Extragalactic Star Formation, ed. R. E. Pudritz & M. Fich (Dordrecht: Kluwer), 25
Panagia, N., & Felli, M. 1975, A&A, 39, 1
Panagia, N., & Macchetto, F. 1982, A&A, 106, 266
Pauldrach, A. W. A., & Puls, J. 1990, A&A, 237, 409
Percy, J. R., et al. 1988, A&A, 191, 248
Prinja, R. K., Barlow, M. J., & Howarth, I. D. 1990, ApJ, 361, 607
Scargle, J. D. 1982, ApJ, 263, 835
Schmidt-Kaler, Th. 1982, in Landolt-Bornstein, New Series: Astronomy and Astrophysics, Vol. 2b (Berlin: Springer-Verlag)
Scholten, G. G. J., de Koter, A., & Lamers, H. J. G. L. M. 1994, A&AS, in press
Scuderi, S., Bonanno, G., Di Benedetto, R., Spadaro, D., & Panagia, N. 1992, ApJ, 392, 201
Spitzer, L. 1978, in Physical Processes in the Interstellar Medium (New York: Wiley)
Taylor, M., Nordsieck, K. H., Schulte-Ladbeck, R. E., & Bjorkman, K. S. 1991, AJ, 102, 1197
Van Gent, R. H., & Lamers, H. J. G. L. M. 1986, A&A, 158, 335